

The first prototype diamond monochromator at the Institut Laue-Langevin

P Courtois^{*1}, **M T Fernandez-Diaz**¹, **G Nenert**¹, **K H Andersen**², **A K Freund**^{1,3}, **S Gsell**⁴, **M Fischer**⁴, **M Schreck**⁴, **P Link**⁵ and **M Meven**⁶

¹ Institut Max von Laue - Paul Langevin, Grenoble, France

² European Spallation Source ESS, Lund, Sweden

³ Via Cordis - Consulting and Movement, Bordeaux, France

⁴ Institut für Physik, Universität Augsburg, Augsburg, Germany

⁵ Forschungs-Neutronenquelle Heinz Maier-Leibnitz (FRM II), Technische Universität München, Garching, Germany

⁶ RWTH Aachen, Institut für Kristallographie, Aachen and Forschungszentrum Jülich GmbH, Jülich Centre for Neutron Science (JCNS), Outstation at MLZ, Garching, Germany.

E-mail: courtois@ill.fr

Abstract. We report on the performance of the first diamond neutron monochromator built at the ILL. It has been designed for the hot neutron diffractometer D9 with the aim of improving significantly the instrument performance in particular for short wavelengths in the 0.3-0.9 Å wavelength range. Diamond crystal plates with dimensions of 1.5 x 1.5 x 0.18 cm³ and an average mosaic spread of 0.15° have been synthesized at the University of Augsburg. They exhibited excellent neutron diffraction properties when examined on a neutron double-crystal test setup. Sufficiently thick diamond elements with a controlled mosaic spread of 0.25° have been obtained by stacking several of these crystals. First tests runs carried out at the ILL confirmed the predicted high reflectivity of the diamond stacks. The diamond prototype monochromator uses the (220) reflection in transmission geometry replacing the Cu (220) monochromator on D9 that has the same *d*-spacing. The final performance studies on D9 showed that the diamond device did not perform better than the original copper crystal. This unexpected result could be explained by significant optical aberrations caused by non-uniformities of both the angular and spatial mosaic distribution in the individual diamond crystals, as revealed by a detailed characterisation study using high-energy X-ray diffraction.

1. Introduction

Thanks to its very favourable crystalline and nuclear properties, diamond offers theoretically the highest performance of all existing materials for neutron monochromator applications [1]. It has a very compact structure with a small unit cell ($a = 3.5668 \text{ \AA}$) composed of 8 carbon atoms having a big coherent scattering length ($b = 0.665 \times 10^{-12} \text{ cm}$) and very low incoherent and absorption cross-sections

* To whom any correspondence should be addressed



Content from this work may be used under the terms of the [Creative Commons Attribution 3.0 licence](https://creativecommons.org/licenses/by/3.0/). Any further distribution of this work must maintain attribution to the author(s) and the title of the work, journal citation and DOI.

for thermal neutrons. At a wavelength of 1.8 \AA $\sigma_{\text{inc}} = 0.001 \times 10^{-24} \text{ cm}^2$ and $\sigma_{\text{abs}} = 0.0350 \times 10^{-24} \text{ cm}^2$, respectively. It has been shown that a sufficiently thick diamond crystal with an appropriate mosaic spread would outperform by far existing materials such as copper and germanium mosaic crystals, especially for the monochromatisation of hot neutrons, in the range of $0.3\text{-}1 \text{ \AA}$ [1,2]. However, when the present project started there we neither crystals of appropriate size available (at reasonable costs) nor existed a concept how to generate a defined mosaic spread in big diamond single crystals. Thus, the controlled synthesis of large area diamond crystals with sufficient thickness and appropriate mosaic spread represented quite a big challenge in material science.

This problem was tackled by a research group at the University of Augsburg that has succeeded in producing mosaic diamond crystals using plasma chemical vapour deposition (MWPCVD). Heteroepitaxial diamond layers are grown in the $\langle 001 \rangle$ direction on a 150 nm thick iridium (001) film coated onto a thin layer of yttria-stabilised zirconia deposited on a silicon (001) wafer [3,4]. The surface of crystal plates is nearly parallel to (100) crystallographic planes, typically a few degrees off while both edges are parallel to (110)-type directions. In the meantime it is possible to obtain good quality crystal plates that are up to 0.18 cm thick with lateral dimensions of $1.5 \times 1.5 \text{ cm}^2$. Neutron double-crystal diffraction studies of a great number of samples has shown a high diffraction efficiency yielding values of the peak reflectivity close to the theoretical predictions [4,5]. The potential of heteroepitaxial diamond crystals suitable for neutron monochromators has thus been demonstrated unequivocally. Following this promising result, we decided to build a full-scale prototype monochromator for the hot neutron single crystal diffractometer D9 at the ILL [6]. It should produce the highest performance ever achieved at short wavelengths and would thus represent a significant improvement for reactor based hot neutron instruments.

In the following sections we report on the design, describe the different steps involved in the construction and report on the performance of the first diamond monochromator.

2. Monochromator layout

The diffractometer D9 is presently equipped with a copper (220) monochromator in transmission geometry composed of 3 flat, 0.8 cm thick mosaic crystal plates characterised by a mosaic distribution of 0.25° . With an active area of $6 \times 6 \text{ cm}^2$, it has been optimised to provide neutrons in the wavelength range from 0.3 to 0.9 \AA . The monochromator is flat in order to achieve polychromatic pseudo-focusing at the sample position according to the geometry of the incoming white beam [6].

The prototype diamond monochromator was designed specifically for D9 to replace the existing copper monochromator with the aim of improving significantly the performance of this instrument [6]. To compare directly both monochromators in terms of neutron flux and resolution, we have chosen diamond crystals with characteristics similar to that of the copper crystals currently used on D9, *i.e.* identical mosaic spread, d -spacing and active area.

3. Neutron diffraction properties of the diamond crystals

To provide the material for the construction of the monochromator, more than 50 diamond crystals were grown at the University of Augsburg. The neutron diffraction properties of all these diamond samples were studied on the double-crystal test instrument T13C at the ILL. A perfect Ge (331) monochromator crystal selected a wavelength of 1 \AA out of a thermal guide tube. The effective neutron mosaic spread was determined as the full width at half height of (220) rocking curves recorded in transmission geometry. The beam cross-section was $0.2 \times 0.2 \text{ cm}^2$. Since the d -spacing of Ge (331) is very close to that of diamond (220), $d_{\text{Ge331}} = 1.296 \text{ \AA} \sim d_{\text{C}^*220} = 1.261 \text{ \AA}$, the double-crystal configuration was parallel and the arrangement nearly dispersion-free. Thus the width of the rocking curve represented directly the mosaic distribution of the sample under study. Moreover, there was no $\lambda/2$ -contamination since the curvature of the thermal neutron guide cuts off neutrons of wavelength below 0.8 \AA . As a result, the neutron reflectivity could directly be derived from the crystal rocking curve as the ratio $R(\theta) = I_r(\theta)/I_0$, where I_0 is the intensity of the direct beam and I_r is the intensity of the reflected beam. The peak reflectivity is the value of $R(\theta)$ in the peak centre.

A typical neutron rocking curve obtained from a 0.18 cm thick diamond crystal is shown in figure 1. The peak reflectivity is close to 34.5% for a FWHM of 0.18°. It corresponds to 80% of the theoretical peak reflectivity calculated from the Darwin model for ideally imperfect mosaic crystals [7]. The origin of the lower reflectivity could be assigned to primary extinction processes and some crystal inhomogeneities [8].

The individual diamond single crystal platelets exhibited high reflectivity, already comparable to that of the best monochromator elements made of copper mosaic crystals despite the fact that their thickness was still significantly below the theoretical optimum. To use the full potential of diamond the thickness of the crystals had to be increased. At the same time, to meet the instrument requirements, it should be possible to tailor the mosaic spread.

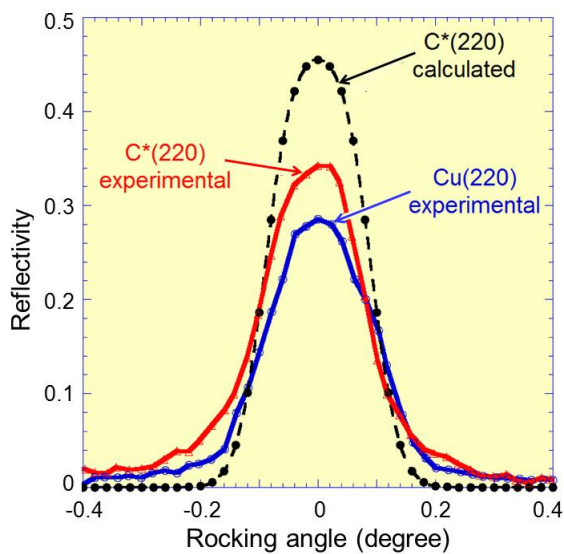


Figure 1. Experimental and theoretical neutron rocking curves at 1 Å of a mosaic diamond (C*) (220) crystal in Laue geometry with a mosaic spread of 0.3° and a thickness of 0.18 cm. For comparison, the experimental rocking curve of the mosaic Cu (220) crystal presently used on D9 as monochromator is shown too.

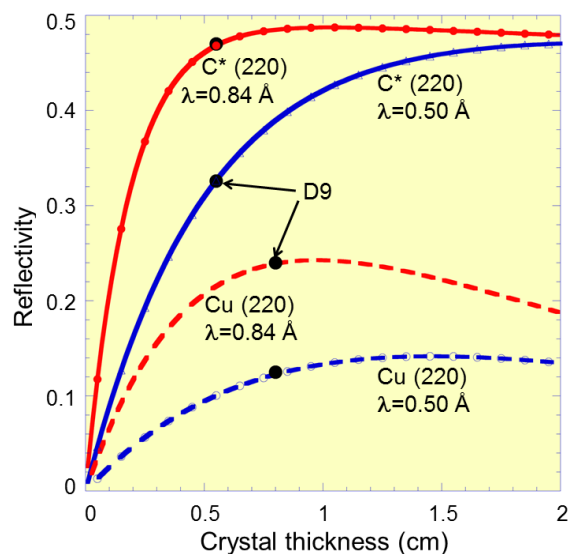


Figure 2. Theoretical neutron peak reflectivity for $\lambda = 0.84 \text{ \AA}$ and 0.5 \AA as a function of crystal thickness for diamond (220) and Cu (220) in Laue geometry with the same intrinsic mosaic spread of 0.25°. The black dots indicate the theoretically predicted peak reflectivities of Cu and C* as crystal monochromators on D9.

4. Composite diamond crystal systems

First of all we consider the crystal thickness needed to maximise the neutron reflectivity of diamond. Figure 2 shows the theoretical peak reflectivity of the diamond (220) reflection in transmission geometry as a function of crystal thickness for two short wavelengths $\lambda = 0.5 \text{ \AA}$ and 0.8 \AA and for an intrinsic mosaic spread of 0.25°. It should be mentioned at this point that due to secondary extinction the neutron mosaic spread defined as the FWHM of the diffraction peak is always a little wider than the intrinsic crystal mosaic spread that is given by the average angular spread of the mosaic blocks or the lattice tilts, see [1]. If not stated otherwise, by mosaic spread we mean the neutron rocking curve width. It can be seen that the peak reflectivity reaches a maximum at an optimum thickness, t_{opt} , that depends on the wavelength, see also [9]. Thanks to the very small capture and inelastic scattering cross-sections of carbon the maximum peak reflectivity approaches 50 % for both wavelengths. The calculations show that the thickness of the crystals available ($t \sim 0.18 \text{ cm}$) is too small with respect to the required values as predicted by the theory: $t_{\text{opt}} \sim 1 \text{ cm}$ at $\lambda = 0.8 \text{ \AA}$ and $t_{\text{opt}} \sim 2 \text{ cm}$ at $\lambda = 0.5 \text{ \AA}$.

At this point it should be mentioned that not only capture and inelastic scattering contribute to the attenuation of the neutron beam, see [10,11]. Because carbon is such a strong scatterer, also multiple

elastic scattering effects competing with the main diffraction process could significantly affect the reflectivity whereas for copper capture and inelastic scattering dominate the attenuation. Taking this fact into account, the optimum thickness would be smaller than the values given above.

Because the synthesis of 1 cm-thick diamond crystals with a mosaic distribution of 0.25° is currently impossible, we decided to build a composite crystal system by stacking several thin diamond crystal pieces of high quality, each piece being slightly misoriented with respect to its neighbour by an angle α [5]. Note that the term *high quality* refers to crystals of type A as defined in the study described in ref. [8]. The effective total mosaic spread of the composite crystal system is the average spread of the n crystal plates plus $n-1$ times the inclination angle between the plates. Besides the optimisation of the effective thickness for a given wavelength, an important advantage of this technique is that the global mosaic distribution of the crystal stack can be tailored: the misorientation angle must not always be constant within each stack but can be varied if required. This technique called *onion peel method* had been successfully employed earlier for producing highly anisotropic copper crystals with a mosaic spread well adapted for neutron monochromators [12]. It works well if the inclination angle is smaller than or equal to the mosaic spread. Otherwise holes will appear on the angular profile.

Due to the limited number of available crystals, the best compromise was a stack consisting of three plates to obtain an effective thickness of 0.55 cm. Such a stack would theoretically outperform a mosaic copper for the monochromatisation of hot neutrons by more than a factor two as shown in figure 2. The angle α was chosen close to 0.05° in order to achieve a global mosaic spread of the stacks close to 0.25° .

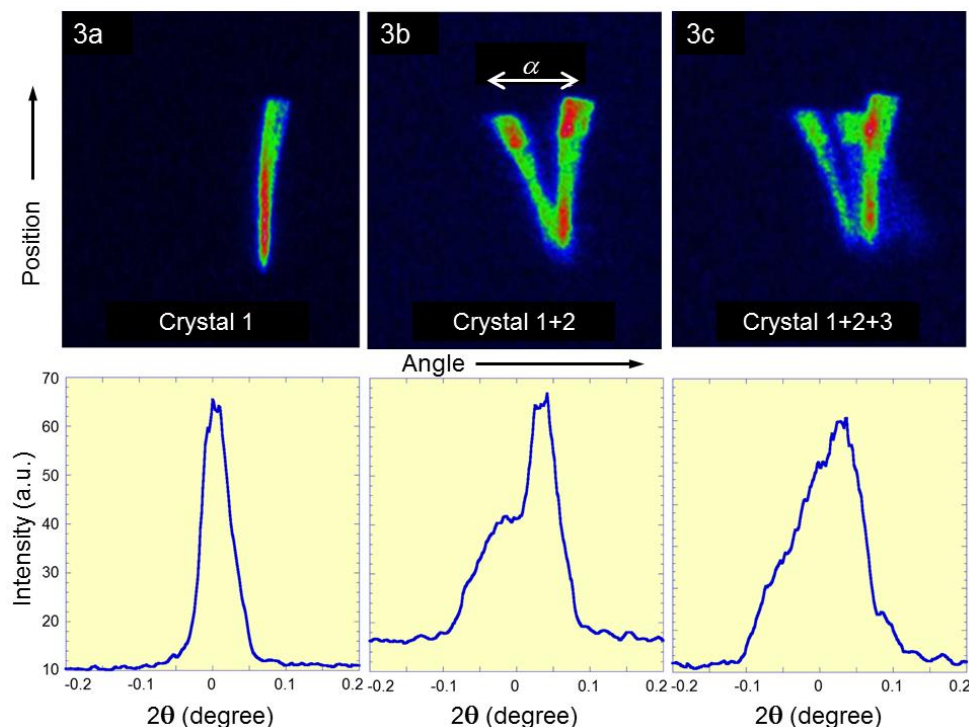


Figure 3. High-energy X-ray diffraction images and peak profiles ($C^*(220)$ reflection) showing the evolution of the mosaic distribution during the stacking procedure. A (left): single crystal plate; b (middle): two-crystal stack; c (right): final stack of three crystals (thickness = 0.55 cm). Note that the angle on the images appears to be bigger than the real one due to the projection.

The production of the composite crystal systems was achieved by using high-energy X-ray diffraction for the precise orientation of the slabs [13]. A high-resolution, two-dimensional detector enabled the visualisation of the diffraction image and the determination of the peak position ($2\theta_0$) with an accuracy of 30 arc seconds. Due to the high energy of hard X-rays (100-450 keV), absorption is small compared to that of standard X-rays (30 keV). As a consequence, the whole bulk of the crystals was probed similar to diffraction experiments with neutrons which offered the opportunity to observe simultaneously diffraction peaks from several crystals stacked together. Thus high-energy, white-beam X-ray diffraction was well suited for assembling stacks of diamond single crystals as described in the next paragraphs.

First, a diamond platelet (crystal 1) was mounted onto the sample table that was equipped with x-y-z translation stages and ω - ϕ - κ angular rotation stages. When placed in the white beam, the crystal diffracted X-rays at the Bragg angle θ_0 according to its orientation (figure 3a). The second crystal attached to an aluminium support (crystal 2) was positioned in front of the first one. A specific and very accurate mechanical support had been developed for this purpose at the ILL consisting of a combination of a goniometer and a translation stage. Then crystal 2 was carefully aligned at the desired angle $\theta_0 + \alpha$, moved very close to the first crystal and then bonded on the latter using a carbon based glue (figure 3b). The translation stage had been specially prepared to keep the precise orientation during the transfer operation. Finally, to complete the stack, the third crystal was aligned and glued onto the second one following the same procedure. This technique allowed a precise orientation of crystallographic planes within an accuracy of 0.01° after gluing. In addition, as shown in figure 3c, such an *in-situ* alignment enabled us to control and optimize the peak profile if necessary.

A total of 16 stacks with a neutron mosaic spread of $0.25^\circ \pm 0.1^\circ$ were successfully prepared using this technique. The reflectivity of the stacks was measured using neutrons on the diffractometer T13C at the ILL giving a typical peak reflectivity of 41% at 1 \AA . Earlier measurements carried out on D9 at smaller wavelengths studying a test stack on the sample position had confirmed its outstanding performance as shown in figure 4. Even with a bigger mosaic spread the peak reflectivity of the diamond stack exceeded by far that of the copper crystal. Note that the rocking curves were wider than the mosaic spread of the crystals under study because their reflection curves were convoluted with the rocking curve of the D9 monochromator that served as first crystal in this double-crystal arrangement.

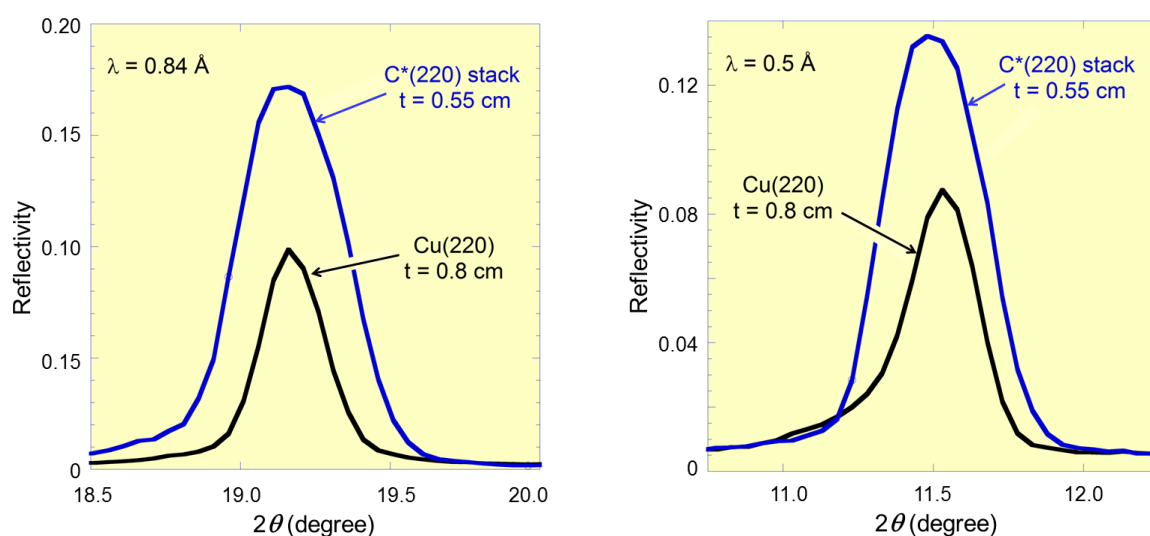


Figure 4. Experimental neutron rocking curves for $\lambda = 0.84 \text{ \AA}$ (left) and 0.5 \AA (right) obtained with a 0.55 cm thick diamond composite system (FWHM = 0.4°) and a 0.8 cm thick Cu (220) crystal (FWHM = 0.25°).

5. Performance of the diamond monochromator

A photograph of the new diamond (220) monochromator consisting of 4 columns of 4 composite crystal stacks that are approximately 0.55 cm thick with a global mosaic distribution close to 0.25° is shown in figure 5. The crystals were glued onto a backing plate cut from a perfect silicon crystal. Again high-energy X-ray diffraction was used to ensure an alignment of the composite systems with an accuracy of better than 0.05° . The monochromator was installed on D9 in February 2013 and tested in the same configuration as the copper device.

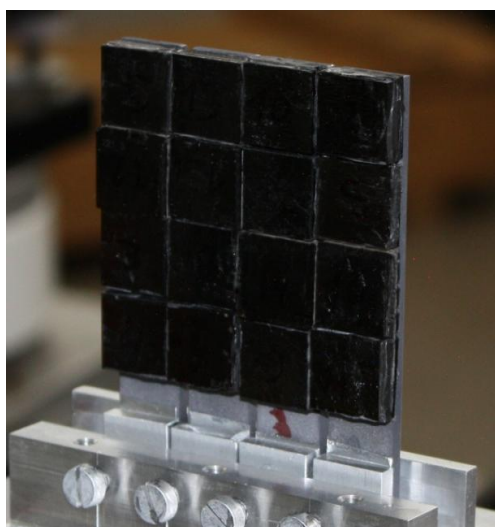


Figure 5. Photograph of the prototype diamond monochromator for the instrument D9 at the ILL.

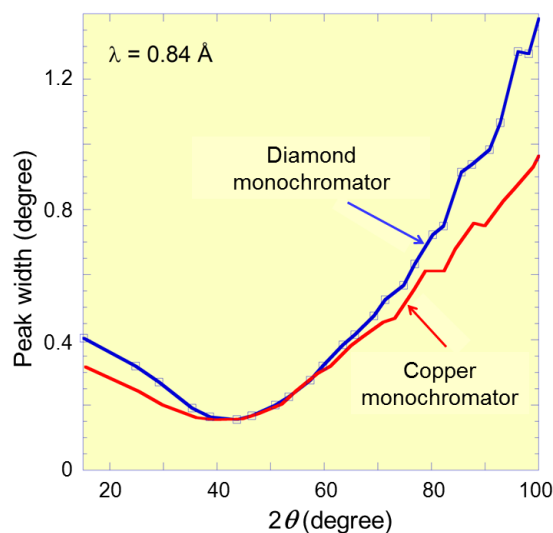


Figure 6. Peak width as a function of scattering angle 2θ measured with a perfect Si crystal on the sample position for $\lambda = 0.84 \text{ \AA}$ with both the diamond and the copper monochromator.

5.1. Neutron flux

The neutron flux at 0.84 \AA and at 0.5 \AA was measured with a neutron monitor at the exit of the D9 monochromator casemate. Surprisingly, it was observed that the diamond monochromator did not provide any gain in neutron flux as compared to copper. The neutron flux was also checked at the sample position by recording the intensity peak profiles of Bragg reflections from a perfect Si crystal as a function of the sample scattering angle 2θ . The integrated peak reflectivity calculated from these measurements confirmed that there was no increase of the neutron flux provided by the diamond monochromator.

5.2. Resolution

Figure 6 shows the resolution curves of the instrument obtained with the diamond and copper monochromators. The two measurements were taken at the same Bragg angle θ_B corresponding to a neutron wavelength of 0.84 \AA . As expected, the minimum of the peak width occurred at a scattering angle 2θ close to $2\theta_B$ and the resolution rapidly decreased for $2\theta > 2\theta_B$ [11]. Moreover, the resolution measured with diamond was inferior to that of copper. From figure 6, with the aid of the well-known Cagliotti formula [15] and by setting $\alpha_1 = \alpha_3 = 0$ (no collimation) and $\alpha_2 = 0.75^\circ$, we obtained $\beta_{Cu} = 0.22^\circ$ and $\beta_{C*} = 0.3^\circ$ where α_n are the opening angles of the beam collimation and β is the neutron mosaic spread, respectively. These values were consistent with mosaic spread measured on T13C from rocking curves of single crystal elements.

6. Crystal analysis and discussion

As already mentioned in the previous section, quite unexpectedly the performance of the prototype diamond monochromator in terms of both neutron flux and resolution did not exceed that of the existing copper crystal. Considering the measured high reflectivity of the diamond stacks that

composed the monochromator, such a low level of performance suggests that an important part of the diffracted neutron beam did not reach the sample position but was dispersed by a non-uniformity of the crystal mosaic structure. On the double-crystal setup at T13C the detector was wide open and always received all the diffracted intensity.

To validate this assumption, a structural analysis of diamond crystals was performed using the high-energy X-ray diffractometer at the ILL [13] that is a powerful tool to investigate crystals defects on the macroscopic scale, *i.e.* in the mm and sub-mm range. A CCD detector permits to visualize structural defects of the crystal lattice, such as mosaicity, sub grains and curvature. For a perfect silicon crystal, the diffraction spot is a straight and narrow line with a width equal to the generator focus size as shown in figure 7a. The height of the spot corresponds to the crystal size. For a non-perfect crystal, the width of the diffraction spot is expanded as a function of both the mosaicity and lattice plane curvature. As an example, the diffraction image in figure 7b obtained from the (220) reflection of a flat copper crystal currently used on D9 shows a nicely uniform mosaic distribution.

Figure 7c represents a typical diffraction image of the (220) reflection from a diamond crystal. The beam size was $2 \times 2 \text{ cm}^2$ so that the full crystal was illuminated by the X-rays. The shape of the image indicates a complex mosaic structure with substantial variations of the peak position in the direction of X-ray scattering (angle 2θ) and also in the vertical direction. Since it is not easy to separate contributions from mosaicity and curvature to the horizontal broadening of the peak width, the crystal was scanned from one end to the other using a narrow beam 0.1 cm wide and 2 cm high so that the effect of horizontal curvature could be neglected. Diffraction images were taken in steps of 0.1 cm along the y-direction of the crystal, see the series of images in figure 8. This scan highlighted relevant information regarding the effect of structural defects in diamond crystals on the reflection properties.

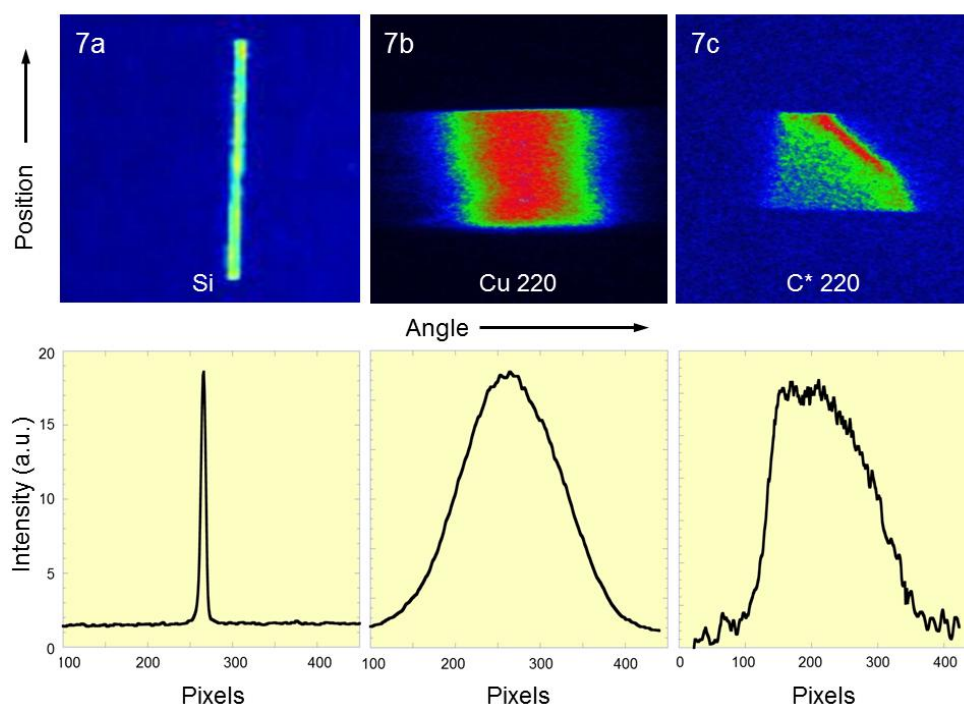


Figure 7. High-energy X-ray diffraction images and peak profiles recorded with a perfect Si crystal (left), with a 0.8 cm thick copper mosaic crystal used on D9 (middle) and with a 0.18 cm thick diamond crystal plate (right). The crystal is fully illuminated by the X-ray beam of cross section $2 \times 2 \text{ cm}^2$.

Indeed a peak shift $\Delta\theta_h$ of 0.15° over the length of the plate was observed along the y-direction which indicated a bending of the lattice planes perpendicular to the $\langle 100 \rangle$ axis. It corresponded to an average radius of curvature of 5.7 m. Such a curvature in diamond crystals had already been reported earlier using neutron and X-ray diffraction [2, 8]. It was confirmed in the present study that most of the diamond crystals exhibited a curvature with a radius in the range from 2 to 5 metres along one (100)-direction. Such a relatively strong curvature can indeed affect the performance of the

monochromator because part of the beam is not fully reflected onto the sample. In fact, in the worst case of defocusing, a horizontally bent, 1.5 cm wide crystal with a radius of curvature of 3.5 m produces a fan of 0.5° that after 3 m flight path broadens the beam by 2.6 cm, much bigger than the sample reception width of about 0.5 cm. Thus the pseudo focusing effect that is an important feature at D9 is seriously reduced. This rough estimation already explains the fact that the observed flux was significantly smaller than that expected for a perfectly flat monochromator crystal.

Even more surprisingly, the diffraction image was inclined with respect to the direct beam (z-direction). This indicated a screw type deformation of the crystal lattice along the vertical $\langle 220 \rangle$ axis. A maximum twist angle of $0.07^\circ/\text{cm}$ ($\Delta\theta_v \sim 0.1^\circ$) was observed at each end of the crystal plate. In addition, this twist was not constant but varied strongly with the y position and even changed sign at y close to -1 mm as revealed by the inclination of the image with regard to the vertical direction. Such a change of sign and thus sense of the twist suggests that the crystal deformation in the perpendicular direction was quite complex.

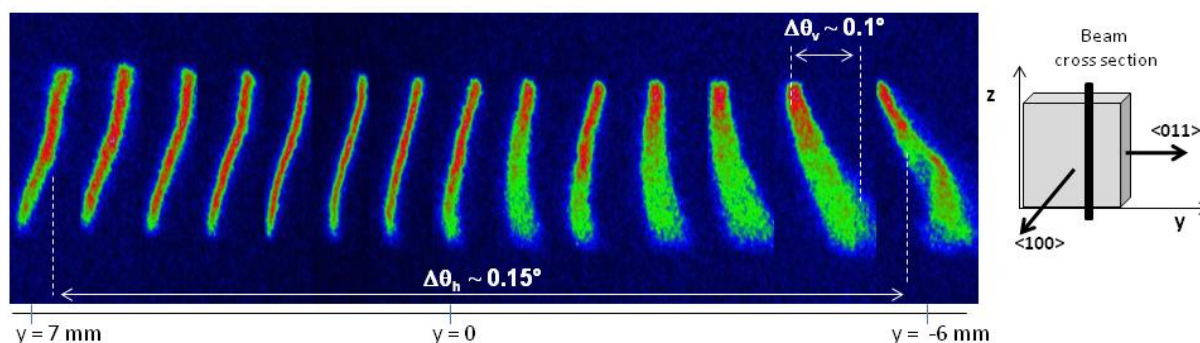


Figure 8. High-energy X-ray diffraction images obtained from a 0.18 cm thick diamond crystal plate with a beam 0.1 cm wide and 2 cm high. The crystal was scanned along the y axis in steps of 0.1 cm.

In addition to these features on the angular scale we observed an important non-uniformity of the spatial mosaic distribution, too. The local (intrinsic) X-ray mosaic spread η_0 was much narrower than the effective mosaic η_{eff} observed from the entire crystal, see figures 7c and 8. The local mosaic distribution η_0 could be determined from the horizontal cross section of the diffraction spot by taking a small region of interest in order to simulate a beam cross section of $1 \times 1 \text{ mm}^2$, *i.e.* 3 pixels high. Thus any broadening of the diffraction spot due to bending or twist deformation could be neglected. At the centre of the diamond plate, we found a mosaic η_0 of as small as 0.05° . Such a small value is to be compared to the 0.22° measured for η_{eff} as determined from figure 7c. Moreover, as illustrated in figure 8, η_0 strongly varied not only between the two ends of the plate in the y direction, but also from the top to the bottom in the z direction. For instance, for $y = 7 \text{ mm}$ η_0 was close to 0.1° , twice the value at the centre of the plate.

It is emphasized once more that the neutron beam geometry on D9 had been designed for a flat monochromator in Laue configuration. In the horizontal direction an intermediate neutron source is imaged onto the sample position if a flat mosaic crystal monochromator is used. Also a deformation of the crystal lattice in the vertical plane affects the monochromator performance dispersing the neutron beam and degrading the instrument performance in terms of flux on the sample, although it is smaller than in the scattering plane.

The maximum acceptable angular deviation on D9 can be estimated by considering the beam geometry. The distance between the monochromator and the sample position is close to 3 metres. Usually a collimator of 1 to 6 mm diameter is mounted at a distance of 2.4 m from the monochromator position. Calculations show that an angular deviation of the diffracting planes of 0.1° would already degrade the neutron flux at the sample position. Indeed, it would induce a spatial deviation of the diffracted beam intensity of the order of 10 mm at the collimator position so that a substantial part of the beam is stopped by the shielding. Such an angular limit is smaller than the typical horizontal peak shift of 0.15° observed for most crystals.

Depending on the sense of curvature (concave or convex), both horizontal and vertical crystal curvatures give rise to under- or overfocusing effects increasing the dilution of neutrons at the sample

position. The screw type deformation also disperses neutrons leading to a loss of otherwise useful flux. Finally, the non-uniform spatial distribution of the mosaicity causes a degradation of the instrument resolution and may cause a non-uniform intensity distribution over the beam spot received by the sample which might affect the quality of the experiments.

7. Conclusion

The first neutron monochromator made of diamond mosaic crystals has been built at the ILL with the aim to upgrade its hot neutron diffractometer D9. This prototype device is composed of 16 crystal stacks 0.55 cm thick and 1.5 x 1.5 cm² wide with an effective mosaic spread between 0.25° and 0.30°. Double-crystal experiments conducted at the ILL have shown that such composite systems would outperform existing copper crystal monochromators by more than a factor 2 for the production of short neutron wavelengths below 1 Å. However, the diamond prototype device did not provide any gain over the copper monochromator in terms of both neutron flux at the sample position and resolution.

Detailed characterisation studies using high-energy X-ray diffraction revealed that most of the diamond crystals exhibited quite complex structural deformations of the lattice planes such as curvature and twist. The spatial mosaic distribution was not uniform as well. These non-uniformities of the spatial and angular mosaic block distribution led to even a slight decrease of the diamond monochromator performance compared to that of the existing copper monochromator with undistorted lattice planes and a homogeneous distribution of the mosaic structure.

Acknowledgements

The authors are grateful to ILL staff members involved in the construction and the alignment of the diamond monochromator: Erwin Hetzler (neutron measurements on T13C), Renaud Silvestre (high-energy X-ray characterisation), Jérémie Baudin-Cavallo and Benoît Mestrallet (crystal mounting). We thank John Archer for his help during the experiments performed on the diffractometer D9.

References

- [1] Freund A K 2009 *J. Appl. Cryst.* **42** 36-42
- [2] Freund A K, Gsell S, Fischer M, Schreck M, Andersen K H, Courtois P, Borchert G and Skoulatos M 2011 *Nucl. Instrum. Methods Phys. Res.* **A634** 28-36
- [3] Gsell S, Bauer T, Goldfuss J, Schreck M, Stritzker B 2004 *Appl. Phys. Lett.* **84** 4541-4543
- [4] Fischer M, Gsell S, Schreck M, Brescia R and Stritzker B 2008 *Diam. Relat. Mater.* **17** 1035-1038
- [5] Courtois P *et al.* 2010 *ILL Annual Report*
- [6] <http://www.ill.eu/html/instruments-support/instruments-groups/instruments/d9>
- [7] Sears V F 1997 *Acta. Cryst.* **A53** 35-46
- [8] Fischer M, Freund A K, Gsell S, Schreck M, Courtois P, Stehl C, Borchert G, Ofner A, Skoulatos M and Andersen K H 2013 *Diam. Relat. Mater.* **37** 41-49
- [9] Freund A K 1985 *Nucl. Instr. Methods Phys. Res.* **A238** 570
- [10] Freund A K 1983 *Nucl. Instr. Methods* **213** 495
- [11] Freund A K 2013 *these proceedings*
- [12] Courtois P, Hamelin B, and Andersen K H 2004, *Nucl. Instr. Methods Phys. Res.* **A529** 157
- [13] Bastie P, Hamelin B and Courtois P 2000 *J.Phys. IV France* **10** 21
- [14] Hewat A W 1975 *Nucl. Instr. Methods* **127** 361
- [15] Cagliotti G and Ricci F P 1962 *Nucl. Instrum. Meth.* **15** 155